Transactions of the **13th International Conference on Structural Mechanics in Reactor Technology** (SMiRT 13), Escola de Engenharia - Universidade Federal do Rio Grande do Sul, Porto Alegre, Brazil, August 13-18, 1995

Elastic-plastic analysis of a three-dimensional defect in a tube subjected to imposed cyclic bending

Chapuliot, S.[1], **Goudet, G.**[1], **Autrusson, B.**[2]
1) Commissariat à l'Energie Atomique, DRN/DMT/SEMT, Gif-Sur-Yvette Cedex, France
2) IPSN/DES/SEGREN, CEN, Fontenay aux Roses Cedex, France

ABSTRACT : The authors propose a numerical simulation by finite elements of a propagation test of semi-elliptical defects subjected to imposed curvature. The analysis is elastic-plastic and represents the first load build-up and one full loading cycle. Stress distribution during the cycle and the opening of the crack are evaluated. A local J calculation is also proposed for a crack front measured on the post-cracked specimen.

1. INTRODUCTION

In order to improve Leak Before Break methods, a numerical study was carried out at the CEA based on propagation tests of semi-elliptical defects, to develop methods for calculating J. The tests, also conducted at the CEA, consisted in subjecting a tube containing an axial, semi-elliptical, external crack, to cyclic ovalization.

This presentation concerns the overall numerical simulation in the elastic-plastic domain. The calculation models the geometry of a defect measured on a mock-up and the initial notch cut in the tube. The crack closure effects is evaluated by modelling one and a half loading cycles and the values of J are given for the first load build-up.

2. GEOMETRY

Figure 1 shows an overall view of the tube. As may be observed, the defect is machined in a weakened section 7.44mm thick. The crack front measured and selected for modelling is define by its depth a = 3.87mm and its width 2.c = 21.62mm.

3. MESH

Contrary of the elliptical transformations [1], a procedure which define both the machined initial notch and the crack front was developed. Only one quarter of the tube is modelled. The complete mesh, shown in Figures 2,3 and 4, is defined by 832 quadratic elements with 15 or 20 nodes, making a total of 4163 nodes.

4. MODEL

The approach often used to simulate fatigue tests is to imposed the loading variation over the cycle, using the cyclic tensile stress-strain low. We suggest another approach here. This consists in simulating one and a half loading cycles, using monotonic tensile curve of the material as constitutive equation. This method is used to identify any closures of the crack during the cycle. A bilinear constitutive equation with kinematic

hardening was adopted. It is shown in Figure 6 in comparison with tensile curve of specimen of the same material.

5. LOADING

During the test, the tube was subjected to a cyclic ovalization. The ration between the minimum and the maximum imposed ovalization was 0.1. The loading is obtained numerically for a uniform vertical displacement of the uppermost generating line of the tube (Figure3). The points corresponding to the extrema of the loading path are noted ❶ ❷ and ❸ in figure 5.

6. LOAD DISPLACEMENT CURVE

The response to the imposed ovalization is shown in Figure 5. During the first load build-up, plasticity appears around the crack for an imposed displacement of 1mm, and then remains localised in the defect section. For this loading level, the plasticity has little effect on the overall behaviour of the structure. After this maximum, for the loading cycle, only a small number of points again undergo plastic flow, although strain hardening is kinematic. The structure remains globally elastic.

7. COMPARISON BETWEEN TEST AND CALCULATION

Several parameters were measured during the test. These including the resultant load, deformations in the internal skin in the defect section, opening crack and ovalizations (Figure 7). The comparison between test and calculation is shown in table 1.

The ovalization and the opening of the crack have been overestimated, and deformations in the internal skin are underestimated. This can be explained by the difference in accounting for the loading in the test and the calculation. Numerical simulation implies a uniform displacement of the generating line, whereas for the test, the loading is obtained by the translation of two rigid jaws, of finite thickness, which grip the tube along its entire length.

8. CRACK OPENING

To identify any closure of the crack, Figure 8 shows the measurement of the crack opening angle for the first two extrema of the loading path and for the entire crack front. This angle illustrates the opening of the crack, but is unconnected with the different CTOD measurements proposed by [2], because it is linked to the size of the elements around the front. The element size, which is constant for the entire crack front, is not sufficient to evaluate this quantity.

Figure 8 shows the absence of any closure. The calculated angle remains constantly positive because the imposed strain during the first load build-up are greater than the variations in the quasi-elastic strains of the cycle. The crack remains open.

9. STRESSES AND STRAINS

The stresses and strains are presented around the crack front for two different nodes lines and for two extrema of the loading path. Since there is virtually no strain hardening during the fatigue cycle, the results at point ❸ are merged with those of point ❶.

Initially, Figures 10 to 12 show the results along the ligament, assuming the origin at the internal skin. In a second time, they present the same parameters calculated along the crack front (Figures 13 to 15). The angle ϕ is represented in Figure 4 as in [1].

9.1. Ligament

- The strains calculated at points ❶ and ❷ vary homothetically. The monotonic increase in strain is a consequence of the imposed curvature.
- Normal stresses calculated at point ❶ have an equivalent form to the strain. At point ❷, due to the strain hardening, they pass through a minimum and then become positive in the internal skin. The stress variation is then considerable and explains why cracks appears during the tests. This was observed by [4] and are related to bending loading.
- The equivalent stress variation has a completely different form. At point ❶ of the loading, it displays a local minimum created by the bending load. Elsewhere, the stresses are relatively uniform, above the elastic limit, revealing significant flow. At point ❷ the form of the stress is far more distributed. The appearance of positive normal stresses generates a peak and two minima.

9.2. along the crack front

- The strains calculated along the crack front have an increasing monotonic form from the notch rote to the outer skin. The is due to the imposed curvature.
- The normal stresses are much more uniform. This form, associated with the strains, reveal a flow and substantial redistribution in the outer skin.
- Contrary to the normal stresses, the equivalent stresses increase from the rote to the edge of the crack. The shape remain the same for both extrema of the loading path.

10. PARAMETER J

The J integral, evaluated by the procedure G(θ) [3], is presented along the front, for the first loading, in Figure 9. Note in this figure that J is highest at the edge. This is consistent with the experimental result which, at the start of propagation, revealed a faster propagation velocity at the edge than at depth. Comparison between equivalent stress and J distributions (Figures 9 and 15) shows that this stress appears to be a decisive parameter to evaluate J. This is not the case for normal stress (Figure 14) which passes through a maximum at the middle of the crack front.

11. CONCLUSION

This article has presented the numerical simulation of a fatigue test. It shows that the overall behaviour of the structure is quasi elastic over the cycle, with no closure of the crack. A detailed analysis of the stress distribution reveals a substantial stress variation in the internal skin, explaining the appearance of fatigue cracks during the tests.

To conclude, the J integral shows that the equivalent Von-Mises stress is a suitable parameter for evaluating J by simplified method.

REFERENCES

[1] I.S Raju and J.C. Newman : Stress intensity factor for a wide range of semi-elliptical surface cracks in finite thickness plates. Eng. Frac. Mech., Vol. 11, pp 817-829.

[2] D.E. McCabe and H.A. Ernst : Crack growth resistance measurement by crack opening displacement methods. Fracture Mechanics, fifteenth symposium.

[3] X.Z. Suo and A. Combescure : On the application of the G(θ) method and its comparison with De Lorenzi's approach. Nucl. Eng. and Design, 135, 1992, pp 207-224.

[4] I. Nonaka : Creep-fatigue crack propagation behaviour in surface cracked plate. SMIRT 11, transactions vol. L (August 1991) Tokyo, Japan.

Fig. 1 : Geometry.

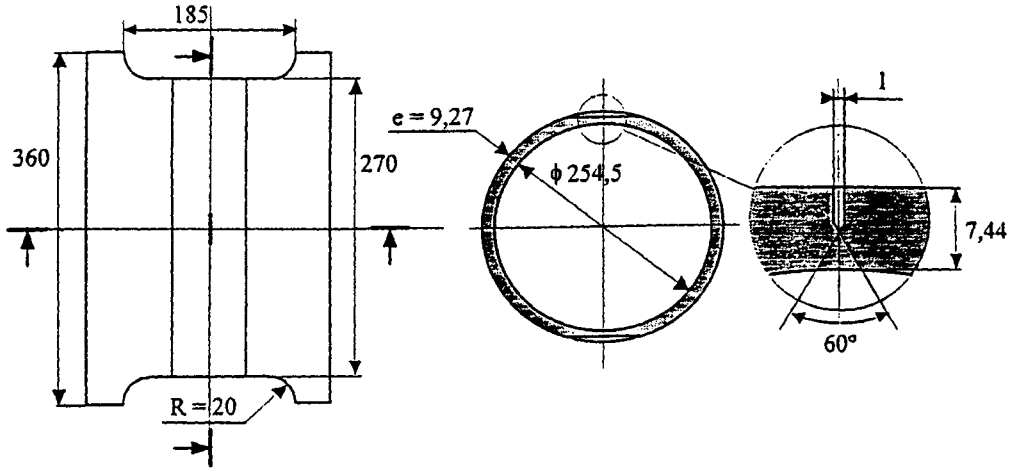

Fig. 2 : Crack front and initial defect.

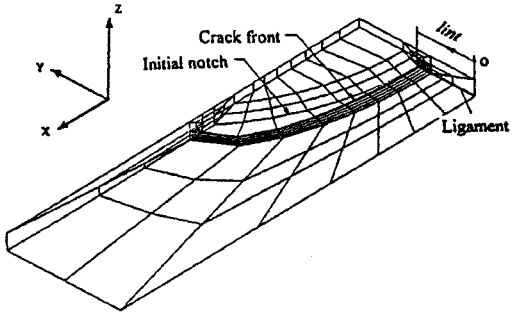

Fig. 3 : Global mesh.

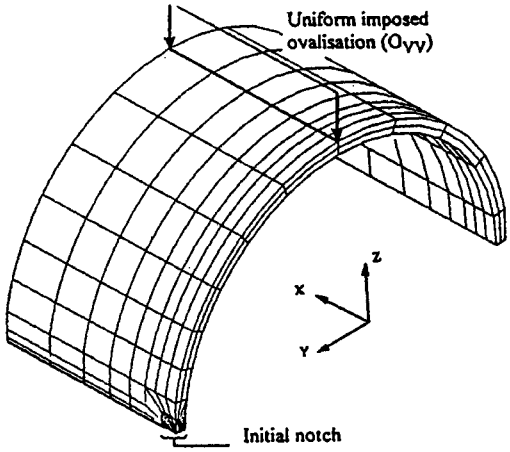

Fig. 4 : Mesh around the crack front.

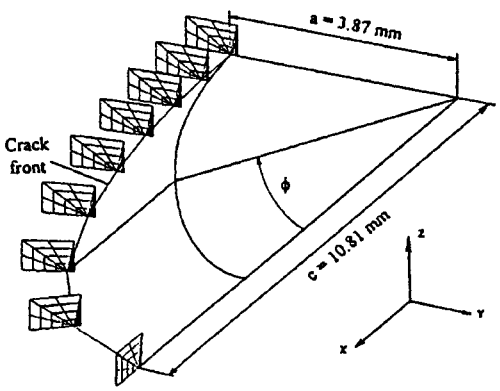

Fig. 5 : Load-displacement curve.

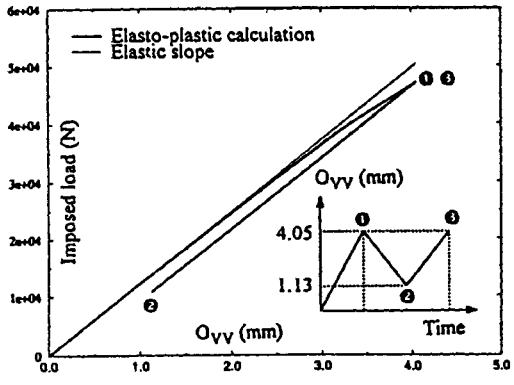

Table 1 : Comparison between calculation and experiment.

	Experiment	Elastic calculation	Point ❶	Point ❷	Point ❸	❸ - ❷
O_{VV} (mm)	2,95	2,95	4,08	1,13	4,08	2,95
O_{VH} (mm)	2,68	2,24	4,11	1,17	4,11	2,94
O_{UV} / h (%)	0,30	0,34	0,58	0,26	0,58	0,32
J5 (%)	0,25	0,23	0,57	0,36	0,57	0,21
J6 (%)	0,23	0,18	0,40	0,22	0,40	0,18
J4 (%)	0,19	0,16	0,31	0,15	0,31	0,16
J7 (%)	0,20	—	0,28	0,13	0,28	0,15
Load (kN)	34	36,4	47,2	11,0	47,2	36,2

Fig. 6 : Stress-strain low.

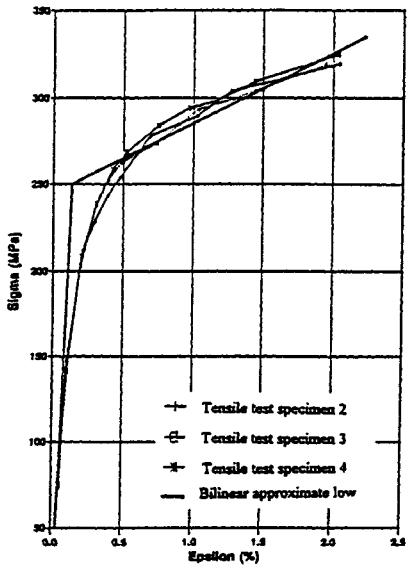

Fig. 7 : Strain gauges and crack opening.

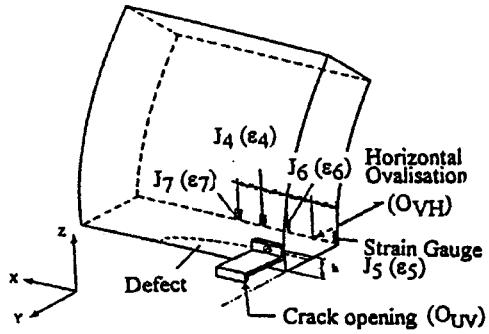

Fig. 9 : J integral along the crack front.

Fig. 8 : Crack opening along the crack front.

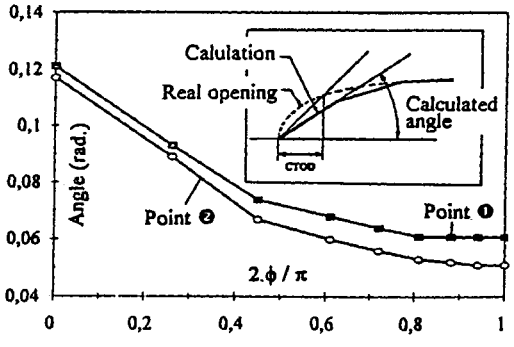

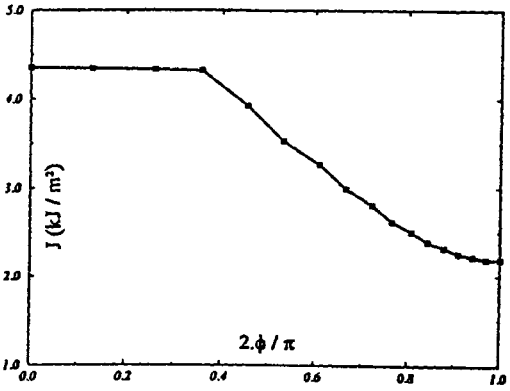

Fig. 10 : Normal strain along the ligament.

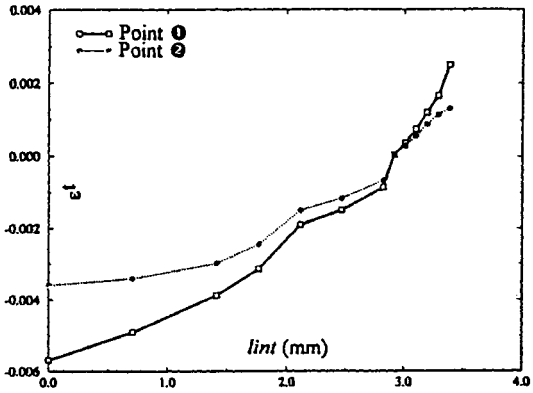

Fig. 13 : Normal strain along the crack front.

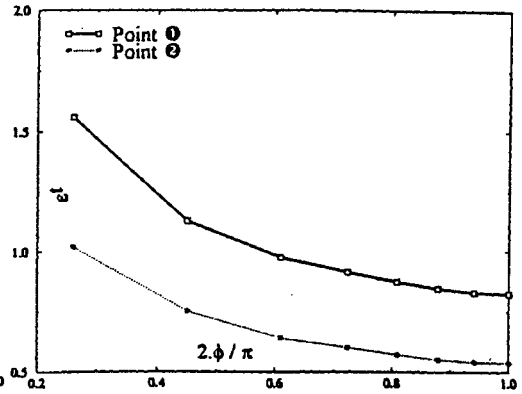

Fig. 11 : Normal stress along the ligament.

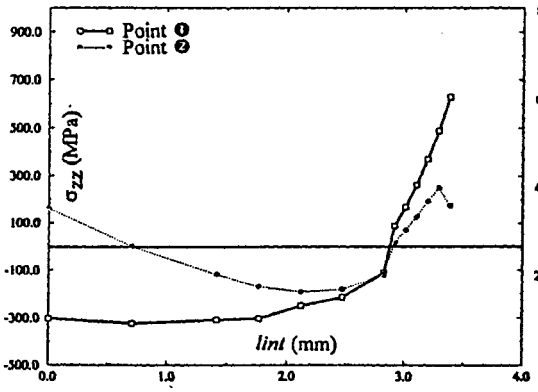

Fig. 14 : Normal stress along the crack front.

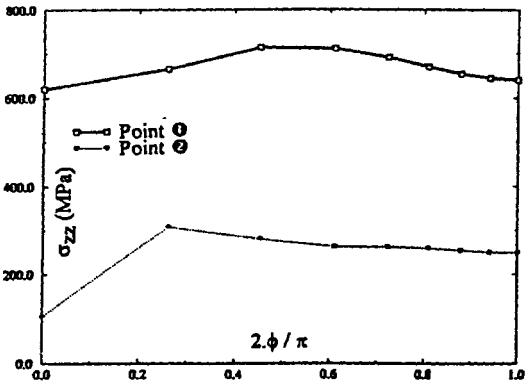

Fig. 12 : Equivalent stress along the ligament.

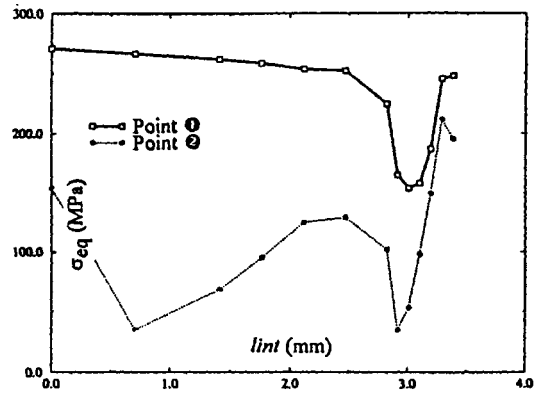

Fig. 15 : Equivalent stress along the crack front.